Rayleigh Scattering Measurements of Fuel Vapor Concentration Fluctuation in a Motored Spark Ignition Engine

F.Q.Zhao, T.Kadota* and T.Takemoto

Department of Mechanical Engineering
Hiroshima University
** Department of Mechanical Engineering*
University of Osaka Prefecture
Mozu-Umemachi
Sakai 591
Japan

ABSTRACT

An experimental study was presented of the measurement of the fuel vapor concentration fluctuation in the combustion chamber of a motored spark ignition engine via the laser Rayleigh scattering. The results showed that the concentration fluctuation consisted of the temporal concentration fluctuation in a specific cycle and cyclic variation of the temporal mean concentration, which could be measured seperately by the present experimental apparatus. It was found that the fuel vapor state could be described clearly by four physical parameters defined in the present investigation which were the ensemble-averaged mean concentration, the cyclic variation of the temporal mean concentration, the ensemble-averaged concentration fluctuation, and the cyclic variation of the temporal concentration fluctuation. It was demonstrated that the mean concentration and the concentration fluctuation increased and reached peaks after which they decreased during intake and compression strokes.

INTRODUCTION

As well known, the mixture formation process in the combustion chamber of a spark ignition (SI) engine has a major impact on the engine performances. Therefore, it is imminent to clarify the mixture formation process in the combustion chamber of an SI engine. But it is very complicated due to the simultaneous occurrence of the random movement of the liquid fuel droplet, its evaporation and the diffusion of the fuel vapor with the laspe of time in the engine combustion chamber, which are also influenced greatly by the engine air flow.

Until now, many investigations have been carried out on the clarification of the engine mixture formation process. To make clear the effect of the air flow on the engine performance, many detailed research works have been reported of the measurements of air flow profile in the engine combustion chamber and the associated turbulence (1)(2)*. For full understanding of the fuel droplet behavior, the droplet number and its size were measured with the applications of laser video imaging system (3) and laser Mie scattering (4). A simulation work of the fuel droplet gasfication in an SI engine was also reported (5). To gain a clear idea of the fuel vapor state, the local mixture strength was measured by using an electromagnetic gas sampling valve (6). The calculation of the time history of the spatially averaged air fuel ratio in the gas phase during cranking at low air temperature on the basis of the measured results of cylinder pressure was also reported (7). Recently, the authors began to measure the fuel vapor concentration profile in the combustion chamber of an SI engine via laser Rayleigh scattering. The mixture formation process during the intake stroke was simulated by the timed or continuous injection of fuel into the steady flow of dust-free dry air through an intake port (8)(9). The measurements of the time history of the fuel vapor concentration in a motored SI engine were also reported (10).

A review of the literature indicates that the knowledge on the physical states of the mixture charged into the combustion chamber is limited for the better understanding of the mixture formation process. Especially, no research work has been reported on the analysis and measurements of the temporal and cyclic fluctuations of the fuel vapor concentration within the combustion chamber of an SI engine.

The present paper is the fourth step of the experimental programme aimed at providing detailed information on the temporal and cyclic fluctuations of the fuel vapor concentration in the combustion chamber of an SI engine with the employment of laser Rayleigh scattering.

THEORETICAL ANALYSIS

When an operating engine is taken into consideration, the application of the conventional concentration fluctuation concepts is complicated by the fact that the mixture state in the combustion chamber changes not only temporally in a specific cycle but also cyclically. Though the overall features of the mixture concentration profiles may repeat each cycle, the details do not because the mean concentration can vary significantly from one cycle to the next. There are both cycle-to-cycle variations in the mean at any crank angle in the cycle, as well as the concentration fluctuations about that specific cycle's mean concentration. This phenomena can be described as follows

---

* Numbers in parentheses designate references at the end of paper.

$$X_f(\theta, i, j) = X_{fT}(\theta, j) + x_{f1}(\theta, i, j) \quad (1)$$

$$X_f(\theta, i, j) = X_{fE}(\theta, i) + x_{f2}(\theta, i, j) \quad (2)$$

where

θ: crank angle

i: the ith of the infinitesimal crank angle interval in the crank angle window Δθ divided by dividing number N_d

j: cycle number

Equation (1) shows that the instantaneous vapor concentration at a specific crank angle in a particular cycle can be divided into two components which are the temporal mean within a narrow window of crank angle as well as the concentration fluctuation about it at a specific crank angle in the specific cycle. Equation (2) shows that the instantaneous vapor concentration in the engine combustion chamber can be expressed as the sum of the ensemble-averaged mean concentration and the variation of the instantaneous concentration about the ensemble-averaged mean concentration. From the above explanation, $X_{fT}(\theta, j)$ can be defined as

$$X_{fT}(\theta, j) = (1/N_d)\sum_{i=1}^{N_d} X_f(\theta, i, j) \quad (3)$$

The ensemble-averaged mean concentration $X_{fE}(\theta, i)$ can be written as

$$X_{fE}(\theta, i) = (1/N_c)\sum_{j=1}^{N_c} X_f(\theta, i, j) \quad (4)$$

where, N_c is the total cycle number. When Eq. (2) is averaged temporally in the crank angle window Δθ, the following equation can be derived

$$X_{fT}(\theta, j) = X_{fET}(\theta) + x_{f2T}(\theta, j) \quad (5)$$

The two components in the right side of this equation can be defined as

$$X_{fET}(\theta) = [\sum_{j=1}^{N_c}\sum_{i=1}^{N_d} X_f(\theta, i, j)]/(N_c N_d) \quad (6)$$

$$x_{f2T}(\theta, j) = (1/N_d)\sum_{i=1}^{N_d} x_{f2}(\theta, i, j) \quad (7)$$

From Eq. (6), it is noted that the ensemble-averaged mean concentration is only a function of the crank angle since the cyclic variation has been averaged out. The difference between the mean concentration in a particular cycle and the ensemble-averaged mean concentration over many cycles is the cyclic variation in mean concentration as shown in Eq. (5). By substituting Eq. (5) into Eq. (1), the following equation can be derived

$$X_f(\theta, i, j) = X_{fET}(\theta) + x_{f2T}(\theta, j) + x_{f1}(\theta, i, j) \quad (8)$$

Thus, it is found that the instantaneous vapor concentration can be split into three components, which are the ensemble-averaged mean concentration, the cyclic variation of the temporal mean concentration, and the temporal concentration fluctuation in the specific cycle. Figure 1 illustrates the breakdown of the instantaneous concentration into an ensemble-averaged component, an individual-cycle mean concentration, and a component which randomly fluctuates in time at a particular crank angle in space in a single cycle. The last component is the conventional definition of the concentration fluctuation. Whether this differs significantly from the variations about the temporal mean concentration depends on whether the cyclic variations are small or large. Figure 1 also shows the definitions of some other physical parameters appearing in the above statements.

The magnitude of the cyclic variation of the temporal mean concentration can be determined from the following equation

$$X_{fR}(\theta) = [(1/N_c)\sum_{j=1}^{N_c}[x_{f2T}(\theta, j)]^2]^{1/2} \quad (9)$$

The temporal concentration fluctuation at a particular cycle is given as

$$x_{f1T}(\theta, j) = [(1/N_d)\sum_{i=1}^{N_d}[x_{f1}(\theta, i, j)]^2]^{1/2} \quad (10)$$

The ensemble-averaged concentration fluctuation can be defined as follows

$$x_{fET}(\theta) = (1/N_c)\sum_{j=1}^{N_c} x_{f1T}(\theta, j) \quad (11)$$

Based on Eq. (9), the cyclic variation of the temporal concentration fluctuation can be expressed as

$$x_{fR}(\theta) = [(1/N_c)\sum_{j=1}^{N_c}[x_{f1T}(\theta, j) - x_{fET}(\theta)]^2]^{1/2} \quad (12)$$

This shows the cycle-to-cycle varying intensity of the temporal concentration fluctuation.

To obtain the temporal mean concentration and the temporal concentration fluctuation at a

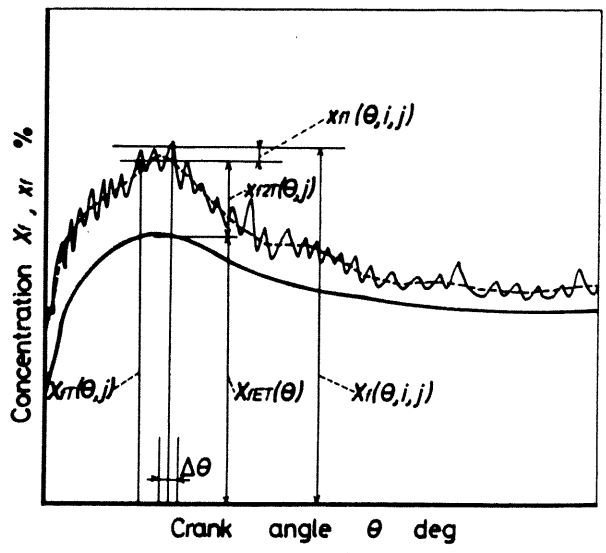

Fig. 1 Definition of physical parameters

particular crank angle in a specific cycle by Eqs. (3) and (10), the crank angle window $\Delta\theta$ should be selected suitably. A preliminary experiment showed that both of the ensemble-averaged mean concentration and the ensemble-averaged concentration fluctuation do not show any appreciable dependence on the crank angle window within the range $\Delta\theta = 1 \sim 5$ degrees. From this result, the crank angle window was determined as 1 degree. In the present research work, the total cycle number is set to be 30.

The theory of laser Rayleigh scattering for the engine study has been described in the previous paper (10).

EXPERIMENTAL PROCEDURES

A schematic diagram of the experimental apparatus is given in Fig. 2. Provided in the measurement was an air-cooled, four stroke-cycle, single cylinder spark ignition engine of which specifications are shown in Table 1. In order to make the optical access feasible, the original engine was modified to permit the installation of an extended combustion cylinder with three glass windows on its side wall. An extended piston was also mounted on the original piston. The engine was driven by a variable speed electric motor. A timing disk was installed to detect the engine crank angle. The fresh air was allowed to pass through a flow meter, a desiccator containing silica gel, an air filter with the pore size of 300 nm and an intake port, and to flow into the combustion chamber. Freon-12 in a tank was allowed to pass through a flow meter and a filter, and to discharge continuously into the intake port from a stainless steel pipe with the inner diameter of 4 mm, which was selected due to its comparatively large Rayleigh scattering cross

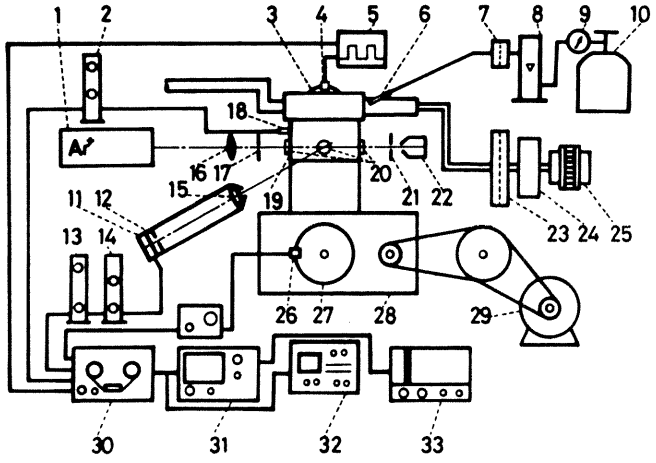

1. Argon laser 2. amplifier 3. light chopper 4. photointerrupter 5. pulse generator 6. injection pipe 7. filter 8. flow meter 9. pressure regulator 10. fuel tank 11. photomultiplier 12. light stop 13. amplifier 14. low pass filter 15. lens 16. lens 17. pinhole 18. pressure transducer 19. extended combustion cylinder 20. glass windows 21. pinhole 22. beam trap 23. air filter 24. desiccator 25. laminar air flow meter 26. photointerrupter 27. timing disk 28. engine 29. motor 30. data recorder 31. oscilloscope 32. signal processor 33. XY recorder

Fig. 2 Experimental apparatus

Table 1 Engine specifications

Type of engine	Four-stroke-cycle spark ignition engine
Cooling system	Air-cooled
Number of cylinder	1
Displacement volume	589cm^3
Bore × Stroke	94 × 85 mm
Compression ratio	8.5(3.1)
Intake valve timing	O:32°BTDC C:68°ABDC
Exhaust valve timing	O:70°BBDC C:30°ATDC
Ignition timing	0°BTDC below 2200rpm 30°BTDC above 4300rpm

section and its noninflammability (8)(9). The cylinder pressure was measured with the use of a pressure transducer.

A 2 W linearly polarized cw Argon laser emitting monochromatic radiation at a wavelength of 488 nm was used as a light source for Rayleigh scattering. A convex lens with the focal length of 300 mm was available to focus the incident laser light on the optical center in the combustion chamber where the measurements of fuel vapor concentration were to be done. Thus, only the small volume of the gaseous mixture was irradiated. To suppress the spurious scattering of incident laser light, two pinholes and a beam trap were provided. The optical detection system consisted of a convex lens with the focal length of 200 mm, a light stop and a photomultiplier (Hamamatsu R928), and was placed at right angle to the incident laser light in the same horizontal plane. This system collected the Rayleigh signal scattered from the gaseous mixture which was contained in a minute volume of the waist diameter of the focused laser light (0.13 mm) divided by a circle with the diameter of 0.25 mm. All the equipments comprising the optical detection system were enclosed in a dark box. The measurements were performed in the subdued light environments. The Rayleigh signal was calibrated with pure Freon-12 gas. The determination of the background light intensity was based on the Rayleigh signal from Helium gas discharged from the stainless steel pipe being subjected to the irradiation of the focused laser light (11). The output electrical signal from the photomultiplier was transmitted through an amplifier and a low pass filter, and was analysed with a signal processor.

Figure 3 shows the detail geometry of the combustion chamber. The injection pipe was fixed at the top portion of the intake port. Three glass windows of the thickness 10 mm and the diameter 35 mm were installed on the side wall of the extended combustion cylinder of the length 87 mm which was mounted between the cylinder head and the cylinder of the original engine. Two of the glass windows were available for transmitting the incident laser light and another was for collecting the Rayleigh

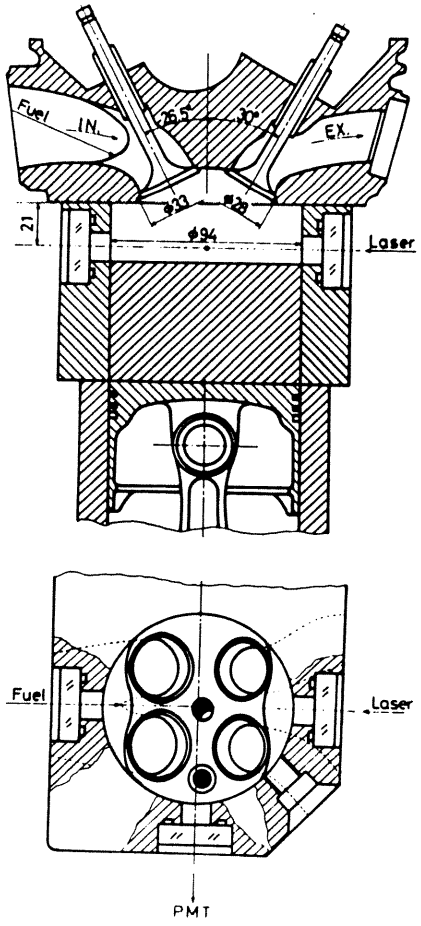

Fig. 3 Combustion chamber

signal. The measurements of fuel vapor concentration were made below one of the spark plugs installed at the center of the cylinder head. The extended piston is flat at its top and the compression ratio is set 3.1.

RESULTS AND DISCUSSIONS

Figure 4 shows the time histories of the ensemble-averaged mean concentration with different air fuel ratios at the engine speed of 750 rpm. It is found that the ensemble-averaged mean concentration X_{fET} increased with the lapse of time, and reached a peak at the crank angle of 60 degrees after which it decreased during the intake and compression strokes. As the intake valve is opened, the rich mixture formed in the intake port is presumed to rush into the combustion chamber. The rich mixture would descend inside the combustion chamber with the piston movement and be diluted due to the turbulent mixing with surrounding air. It is probable that the above process would result in the phenomena shown in Fig. 4. It is also found that the fuel vapor concnetration at the end of the compression stroke is almost the same as the one corresponding to the supplied air fuel ratio. This shows that at this time the Freon-12 vapor has mixed with the air uniformly. From Fig. 4, it is noted that the time history of the fuel vapor concentration during intake stroke is similar to the results with the liquid fuel injection (10). The fuel vapor concentration with liquid fuel injection

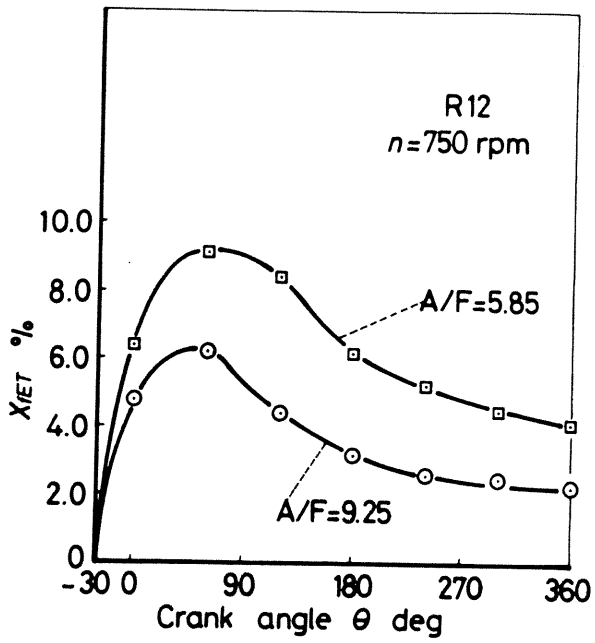

Fig. 4 Ensemble-averaged mean concentration at different air fuel ratios

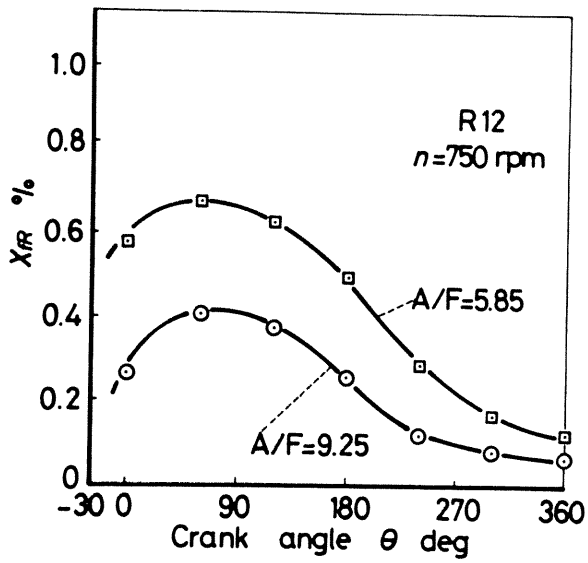

Fig. 5 Cyclic variation of temporal mean concentration at different air fuel ratios

showed no change or a slight increase during the compression stroke, which is different from the results shown in Fig. 4. It is likely that the evaporation of liquid fuel and the dilution of the generated fuel vapor due to the turbulent mixing proceed simultaneously leading to no change or a slight increase of the fuel vapor concentration during the compression stroke when liquid fuel is supplied.

Figure 5 shows the cyclic variation of the temporal mean concentration at different air fuel ratios in the experimental conditions of Fig. 4. It is shown that the cyclic variation of the temporal mean concentration X_{fR} changed with the crank angle, and reached a peak at the crank angle of 60 degrees during the intake stroke. This crank angle is almost the same as the one when the

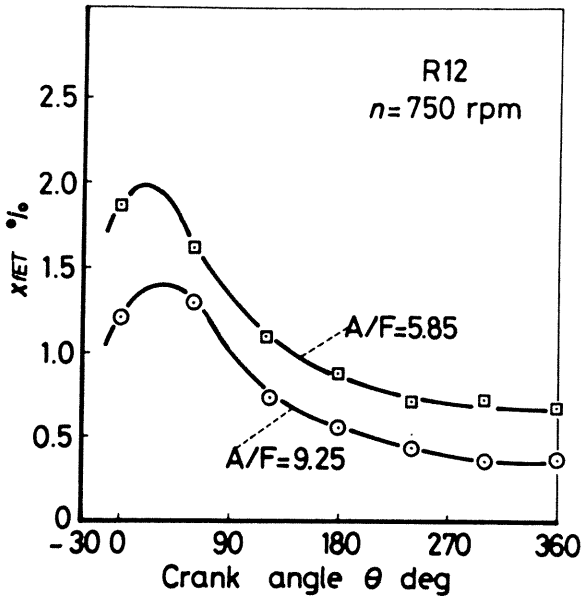

Fig. 6 Ensemble-averaged concentration fluctuation at different air fuel ratios

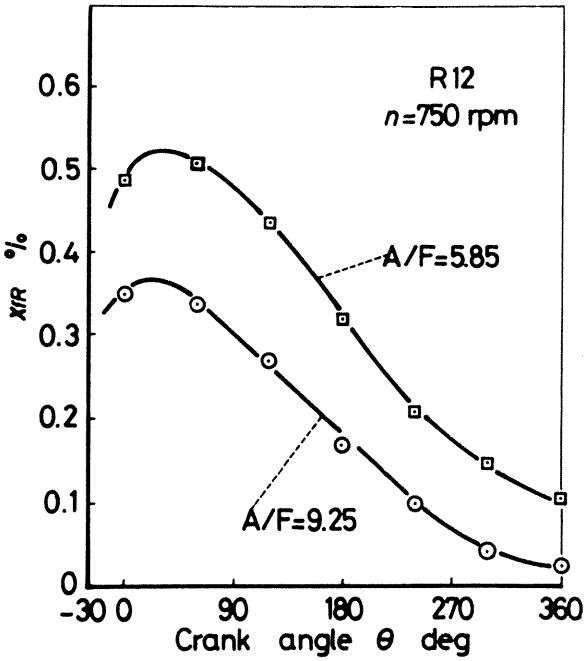

Fig. 7 Cyclic variation of temporal concentration fluctuation at different air fuel ratios

ensemble-averaged mean concentration reached a peak. It is also evident that X_{fR} increased with the decrease of the air fuel ratio. Figure 6 demonstrates the time histories of the ensemble-averaged concentration fluctuation at different air fuel ratios. It is found that x_{fET} also showed a peak during the intake stroke. But the appearance of this peak is a little earlier compared with those of X_{fET} and X_{fR}. It is also found that the ensemble-averaged concentration fluctuation increased with the decrease of air fuel ratios. Comparing the peak values shown in Figs. 4, 5, and 6, it is clear that the cyclic

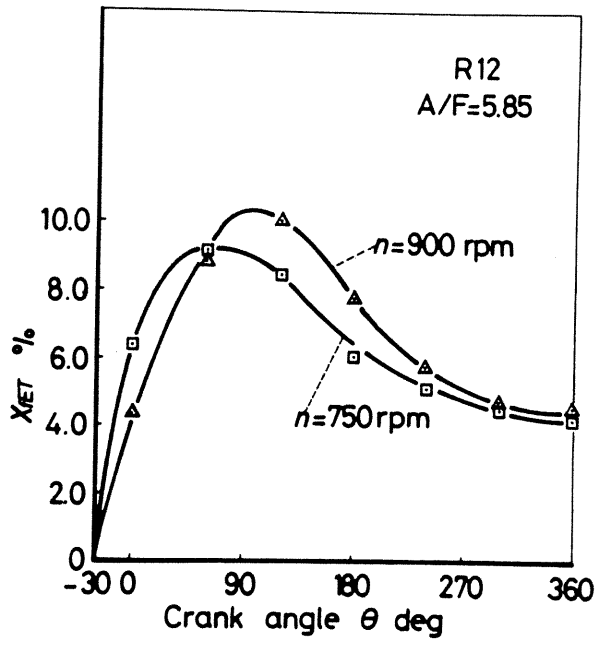

Fig. 8 Ensemble-averaged mean concentration at different engine speeds

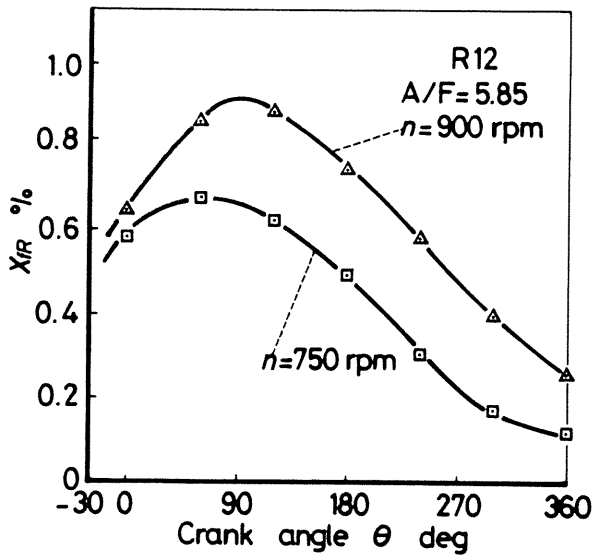

Fig. 9 Cyclic variation of temporal mean concentration at different engine speeds

variation of the temporal mean concentration is about 7% of the ensemble-averaged mean concentration, and nearly 1/3 of the ensemble-averaged concentration fluctuation. The cyclic variations of the temporal conentration fluctuation at different air fuel ratios are shown in Fig. 7. It is found that the cyclic variation of the temporal concentration fluctuation is too large to be neglected when the temporal concentration fluctuation is taken into consideration.

Figures 8, 9, 10 and 11 show the effect of engine speed on X_{fET}, X_{fR}, x_{fET} and x_{fR}. It is shown that the peaks of the above pour physical parameters increase slightly, and the crank angles at their appearances were delayed with the

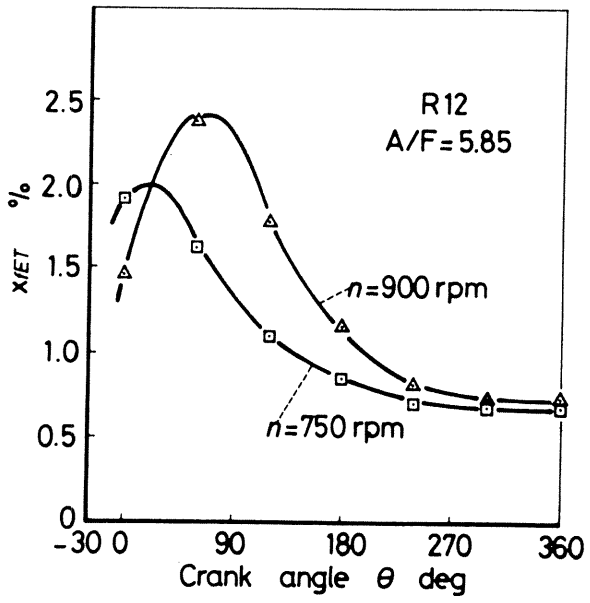

Fig. 10 Ensemble-averaged concentration fluctuation at different engine speeds

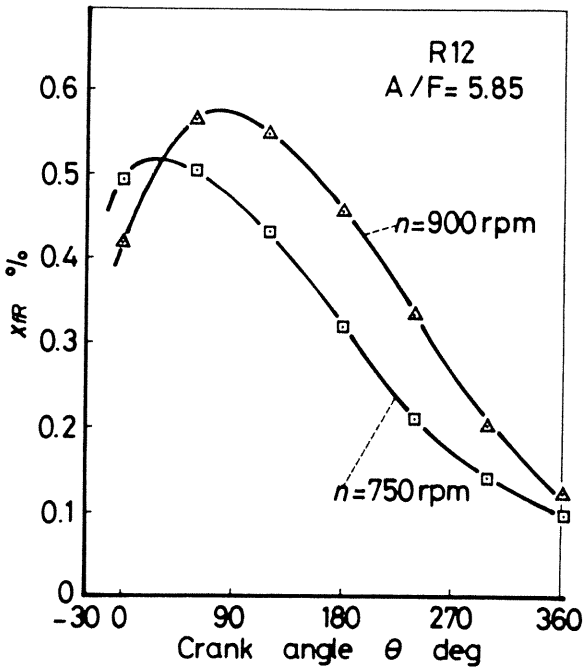

Fig. 11 Cyclic variation of temporal concentration fluctuation at different engine speeds

increase of the engine speed.

CONCLUSIONS

From the present work, the following conclusions are derived.

(1) The concentration fluctuation consists of the temporal concentration fluctuation and the cyclic variation of the temporal mean concentration. The present experimental apparatus is effective to seperate and determine them. In the present experimental condition, the former is larger than the latter.

(2) The ensemble-averaged mean concentration and the ensemble-averaged concentration fluctuation show peaks during the intake stroke after which they decrease during the intake and compression strokes. The appearance of the peak of the latter is earlier than that of the former.

(3) The ensemble-averaged mean concentration and temporal concentration fluctuation increase with the decrease of the air fuel ratio in the whole range of the crank angle.

(4) With the increase of the engine speed, the peaks of the ensemble-averaged mean concentration, the cyclic variation of the temporal mean concentration, the ensemble-averaged concentration fluctuation and the cyclic variation of the temporal concentration fluctuation increase slightly, and the crank angles at their appearances are delayed.

ACKNOWLEDGEMENT

The authors wish to express their gratitude to Suzuki Motor Co., Ltd. for supplying the test equipment.

REFERENCES

1. O. W. Peters, "Conditionally-Sampled Velocity and Turbulence Measurements in a Spark Ignition Engine", Combust. Sci. Technol., Vol.36 pp.301-317, 1984.

2. J. B. Heywood, "Fluid Motion Within the Cylinder of Internal Combustion Engines - The 1986 Freeman Scholar Lecture", J. Fluid. Mech., Vol.109/3, March 1987.

3. B. D. Peters, "Laser Video Imaging and Measurements of Fuel Droplets in a Spark Ignition Engine", Paper C81/83, Presented at the Conference on Combustion in Engineering, IME, Oxford, England, April 11-14, 1983.

4. T. Kadota, S. Mizutani, C. Y. Wu and M. Hoshino, "Fuel Droplet Size Measurements in the Combustion Chamber of a Motored SI Engine via Laser Mie Scattering", SAE Paper 900477, 1990.

5. X. Q. Liu, C. H. Wang and C. K. Law, "Simulation of Fuel Droplet Gasification in SI Engine", Trans. ASME, J. Engng. for Gas Turbines and Power, Vol. 106, pp. 849-853, 1984.

6. A. A. Quader, "The Axially-Stratified-Charge Engine", SAE Paper 820131, 1982.

7. Y. Nakajima, T. Saito, Y. Takagi, K. Katoh and T. Iijima, "The Influence of Fuel Characteristics on Vaporization in S.I. Engine Cylinder during Cranking at Low Temperature", SAE Paper 780612, 1978.

8. T. Kadota, "The Application of Laser Rayleigh Scattering to the Local Mixture Strength Measurements in SI Engine during Intake Stroke", SAE Paper 872151, 1987.

9. T. Kadota, F. Q. Zhao and H. Tsuzaki, "Laser Rayleigh Scattering Measurements of the Fuel Vapor Concentration in the Combustion Chamber of SI Engine", Paper presented at The 5th Int. Pacific Conf. Auto. Engng., Beijing, China, November 5-11, 1989.

10. T. Kadota, F. Q. Zhao and K. Miyoshi, "Rayleigh Scattering Measurements of Transient Fuel Vapor Concentration in a Motored Spark Ignition Engine", SAE Paper 900481, 1990.

11. D. C. Fourgette, R. M. Zurn and M. B. Long, "Two-Dimensional Thermometry in a Turbulent Nonpremixed Methane Hydrogen Flame", Combust. Sci. Technol., Vol. 44, pp. 307-317, 1986.